Structural and optical properties of low-density and In-rich InAs/GaAs quantum dots

Structural and optical properties of low-density and In-rich InAs/GaAs quantum dots

B. Alloing,[a] C. Zinoni, L. H. Li, and A. Fiore
Quantum Devices Group, Institute of Quantum Electronics and Photonics, Ecole Polytechnique Fédérale de Lausanne, CH-1015 Lausanne, Switzerland

G. Patriarche
Laboratoire de Photonique et de Nanostructures, LPN/UPR 20-CNRS, route de Nozay, 91460 Marcoussis, France

(Received 28 August 2006; accepted 9 November 2006; published online 26 January 2007)

Self-assembled InAs/GaAs quantum dots have been grown at very low InAs growth rate in order to form sparse and large quantum dots (QDs) emitting in the near infrared (1300–1400 nm), for application as single-photon sources. The structural and optical properties of these QDs as a function of the growth rate were systematically investigated. The QDs grown at the lowest rate ($\sim 10^{-3}$ ML/s) present a very low dot density ($\sim 2\times 10^{8}$ dots/cm^2), high In content, and good size homogeneity. Photoluminescence and time-resolved photoluminescence measurements performed at different powers and temperatures provide information on their luminescence efficiency, and on the recombination processes occurring in the low-density QDs as compared to higher densities. © *2007 American Institute of Physics*. [DOI: 10.1063/1.2427104]

I. INTRODUCTION

The optimization of growth parameters of self-assembled quantum dots (QDs) has been focused first on the realization of low-threshold lasers. More recently, it has been shown that QDs can be efficiently used as single-photon emitters for quantum cryptography applications[1–3] and growth efforts have been devoted to the fabrication of samples with low dot density to perform single dot spectroscopy. While fiber-based quantum communication applications require an emission wavelength in the 1300 or 1550 nm transmission window, most studies have concentrated on QDs emitting in the $\lambda < 1000$ nm range. This is due to the lower sensitivity of detectors and also to the difficulty of growing sparse and large enough QDs emitting in this spectral region. Until now, microphotoluminescence experiments using InAs/InP QDs have been performed at 1.5 μm (Refs. 4–6) and antibunching experiments have been carried out at 1.3 μm on InAs/GaAs QDs.[7,8] The growth method used in Ref. 7 results on a bimodal distribution of QDs, including sparse and large QDs emitting at 1300 nm. We have recently demonstrated[9] the use of a very low growth rate, as previously suggested,[10] to obtain a single distribution of low-density QDs (LDQDs) emitting at 1.3 μm with a very good size uniformity and high efficiency. Clean exciton-biexciton dynamics,[9] antibunching,[8] and electroluminescence from single QDs (Ref. 11) were observed, making these QDs promising candidates for single-photon sources at 1300 nm.

However, the attractive characteristics of LDQDs (low density and large size) can also affect their radiative efficiency and their thermal stability. Specifically, carrier capture from the wetting layer (WL) to LDQDs is expected to be less efficient, potentially leading to accumulation of carriers in the WL and reducing luminescence efficiency. Moreover, the large size and In content may result in the presence of dislocations. The purpose of this study is to investigate the structure and the optical properties of these LDQDs by comparison with QDs grown under higher growth rates combining different characterization methods such as atomic force microscopy (AFM), transmission electron microscopy (TEM), and photoluminescence (PL) measurements. LDQD size is very homogeneous and larger than usually observed on higher density QDs. A study of growth conditions and an estimation of the In desorption rate show that LDQDs are formed under an InAs growth rate close to the minimum value for which two dimensional-three dimensional (2D-3D) transition occurs. In spite of such limit growth condition, LDQDs exhibit a good luminescence efficiency. While no capture bottleneck has been evidenced even in the lowest QD densities, the presence of WL carriers is observed to play a role in the QD PL dynamics. Finally, LDQDs show a good thermal stability and a temperature dependence of the carrier lifetime similar to what has already been observed on higher density samples.

II. METHODS

The samples are grown by solid-source molecular beam epitaxy on (001)-oriented semi-insulating GaAs substrates. As reported previously[9] we use a combination of ultralow InAs growth rate (<0.002 ML/s) and InGaAs capping layer to obtain LDQDs emitting at 1.3 μm at low temperature. To evaluate the influence of these two parameters, AFM and PL measurements have been performed on a series of samples grown with different InAs growth rates. QDs were obtained by depositing 2.1 ML (monolayers) of InAs on a GaAs buffer, at 505 °C under a background pressure of 5×10^{-7} mbar corresponding to an As_2 molecular flux on the wafer about 4×10^{14} molecules/cm^2 s. We varied the InAs

[a]Electronic mail: blandine.alloing@epfl.ch

growth rate in the range of 0.0012–0.16 ML/s. We determined such values by observing the 2D-3D transition by reflection high-energy electron diffraction (RHEED). Assuming that the critical thickness is 1.7 ML±0.1 ML (Refs. 10, 12, and 13) and depends weakly on the growth rate,[14,15] a value of InAs growth rate can be deduced with an accuracy estimated at 10%. After InAs deposition, samples used for AFM were cooled immediately under As overpressure. For PL investigations, InAs QDs were capped by 100 nm thick GaAs layer. Under the same growth condition, a sample was also grown at low growth rate (0.0015 ML/s), with 5-nm-thick $In_{0.15}Ga_{0.85}As$ capping layer to test the influence of the capping layer. Two different In cells were employed for the growth of QDs and InGaAs capping layer so that a growth rate as high as 0.8 ML/s could be used for the growth of the InGaAs capping layer. To preserve luminescence efficiency of the QDs, the growth temperature during capping layer deposition was kept around 505 °C for all samples.

PL measurements were performed using a Ti:sapphire laser tuned to 780 nm in order to excite carriers in the GaAs surrounding the QDs. Luminescence is dispersed in a 1 m focal lens spectrometer equipped with a linear array of InGaAs detectors. Time-resolved photoluminescence (TRPL) measurements were performed using a pulsed diode laser emitting at 750 nm with a repetition rate of 1 MHz, and focused to a 4 μm spot on the sample with a microscope objective. Emission is collected with the same objective and coupled into a single mode fiber. An idQuantique single-photon avalanche photodiode is used together with a correlation card to provide time-correlated fluorescence spectroscopy with 600 ps resolution.[8]

III. STRUCTURAL CHARACTERIZATION

AFM and TEM techniques have been used to study the evolution of QD morphology with InAs growth rate and to distinguish the different growth mechanisms involved in QD formation. In the following we will make the distinction between the In deposition rate R_{dep} and the InAs growth rate R_G: The In deposition rate is related to the In flux F and represents the amount of incident In atoms coming on the substrate, whereas the InAs growth rate, measured by the RHEED, represents the effective amount of material grown on the substrate. As it is difficult to directly measure the low In fluxes used in this work, one value, F_0, of In flux was obtained at high In cell temperature by extracting the measurement results of x-ray diffraction, and then extrapolated to other cell temperatures with the relation: $F = F_0 \exp(E_{In}/kT_{In})$ with E_{In} the In vaporization energy and T_{In} the In cell temperature. Figure 1(a) shows the variation of R_G (as measured from the 2D-3D transition time); with F, we observe that the relation is linear for $R_G > 0.002$ ML s^{-1}. Figure 1(b) presents the dot density measured by AFM for different In fluxes. At fixed growth temperature and pressure, a dot density as low as 2×10^8 dots/cm^2 is obtained when the In flux is reduced down to 10^{12} cm^{-2} s^{-1} (corresponding to an InAs growth rate of 0.001 ML/s). In this general trend, three distinct regimes are visible: The first regime appears

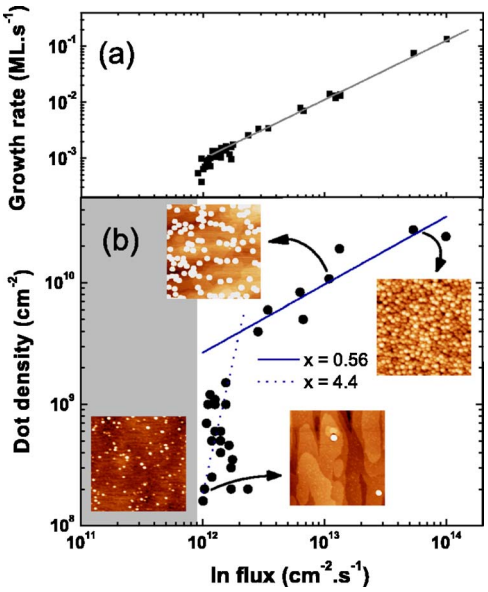

FIG. 1. (Color online) (a) InAs growth rate measured by RHEED under a substrate temperature of 505 °C as a function of In flux. The solid line represents a linear fit. (b) QD density, as measured from AFM images, as a function of In flux. AFM images are done on a 1×1 μm^2 area. The solid and dotted lines show the flux dependence of the dot density fitted by the relation $N=\alpha F^x$, with $x=0.56$ and $x=4.4$, respectively. Gray area represents the region where no nucleation is observed.

for In flux $>3\times10^{12}$ cm^{-2} s^{-1}. The QD density exhibits a dependence on the growth rate following the standard nucleation theory and can be fitted by the relation[16,17] $N=\alpha F^x$. The slight difference between the exponent that we observe, $x=0.56$, and those predicted by theory can be attributed to the influence of the elastic energy which is not taken into account in the model of Refs. 17 and 18. However, this fit cannot be used for $F<3\times10^{12}$ cm^{-2} s^{-1}: QD density decreases abruptly and the fit provides a value of $x=4.4$ in this region. As predicted by Ref. 18, this steeper decrease of the density could be related to the increasing relative contribution of In desorption: as the desorption rate approaches the deposition rate, the number of adatoms available for nucleation decreases. QDs with low areal density $\sim1-10$ μm^{-2} and large size (the height of uncapped QDs is estimated around 12 nm by AFM) are formed in these conditions. Finally, a third regime occurs for In flux lower than 10^{12} cm^{-2} s^{-1} (indicated by the gray area): islanding transition cannot be observed on the RHEED. AFM measurements performed on these samples show a high density (60×10^8 dots/cm^2) of islands, with a significantly smaller size (3 nm) than those grown at a higher growth rate. These small QDs may have been formed during the cooling process of the sample after growth since we do not observe any luminescence signal on a similar sample, capped by a GaAs layer after InAs deposition. This has been attributed to the arsenic condensation during the substrate cooling.[19] We suppose that under these growth conditions, the In desorption rate is comparable to the deposition rate, preventing the onset of nucleation.

In order to compare quantitatively the In desorption rate R_{des} with the deposition rate R_{dep}, we used RHEED to study formation of QDs at different growth temperatures. It is es-

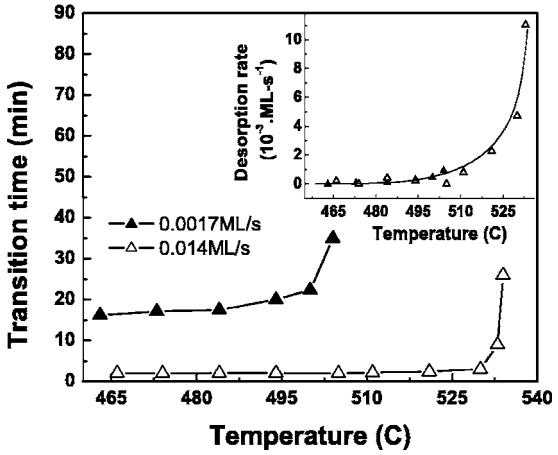

FIG. 2. Evolution of 2D-3D transition time with growth temperature for two In fluxes corresponding to InAs growth rates of 0.0017 and 0.014 ML/s at 470 °C. Inset: Evolution of deduced desorption rate as function of growth temperature; the solid line is a guide to the eye.

tablished that in InAs/GaAs system, intermixing with Ga from the substrate and In desorption are involved in QD formation. The effect of these mechanisms depends strongly on the growth parameters and becomes more significant with increasing growth temperature. We have measured by RHEED the 2D-3D transition time θ for different growth temperatures at two In fluxes (corresponding to InAs growth rates of 0.0017 and 0.014 ML/s at a 470 °C growth temperature). The results are presented on Fig. 2. We observe that θ has a temperature-activated behavior, increasing strongly above a critical temperature, which depends on the InAs growth rate. Since negligible intermixing has been reported for low growth rates[10,20] we attribute this strong increase to In desorption. In these conditions, the growth rate R_G can be expressed as $R_G = R_{dep} - R_{des}$. As θ is almost constant in the 460–480 °C, desorption rate is negligible in this region and a R_{dep} value can be estimated, independent of growth temperature. R_{des} as function of growth temperature can then be deduced, its evolution is presented in the inset of Fig. 2. We note that at 500 °C the desorption rate value reaches approximately 0.0005 ML/s and is in the same range as the In deposition rate, which is used for LDQD growth. This explains the very long transition time at this growth temperature. Furthermore, in the 500 °C region, R_{des} is very sensitive to the growth temperature which results in the dispersion in QD density, as shown in Fig. 1(b). Moreover this value is very close to the minimum value of InAs growth rate above which it is still possible to observe the 2D-3D transition by the RHEED.

We then investigated the morphology of the LDQDs. AFM images show a slight increase of the QD size with a decreasing growth rate. In order to precisely determine the QD dimensions, TEM measurements were performed on two samples containing LDQDs grown at the same growth rate (0.0015 ML/s) with GaAs and InGaAs capping layers. Figure 3 shows cross-sectional (002) dark-field TEM images of the QDs which present a lens shape with higher dimensions than usually observed: 7.5 nm height for QDs capped by GaAs and 10 nm for those capped by InGaAs. These values are larger than the typical height around 5 nm for QDs

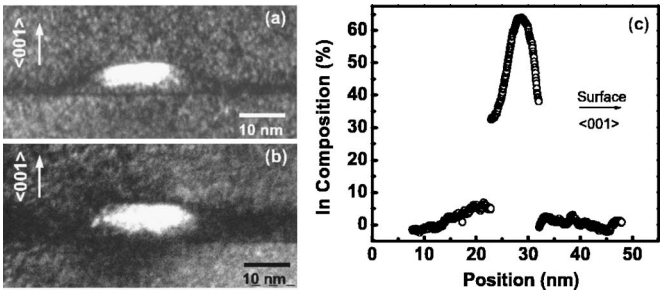

FIG. 3. (002) Dark-field images of QDs grown at low InAs growth rate (0.0015 ML/s) and capped by (a) GaAs and (b) InGaAs. (c) In composition variation in the QDs capped by InGaAs in the ⟨001⟩ direction.

grown at higher InAs growth rate.[21–23] Depending on the capping layer, the morphology of the 2D layer (WL +capping) surrounding the QDs is quite different: uniform for GaAs-capped QDs, the 2D layer for InGaAs-capped QDs appears on the contrary very thick (about 10 nm) close to the QDs and becomes thinner (7.6 nm) at longer distances. To estimate the In composition distribution, we used the technique proposed in Refs. 24 and 25 which allows the estimation of In content from TEM contrast in dark-field (002) images, with a spatial resolution higher than 2 ML. Figure 3(c) shows the In composition profile of the QDs capped by InGaAs along the ⟨001⟩ direction, through the QD center. QDs present a strong In gradient with a maximum In composition of 65% in the center of the dots and 35% at the bottom. The In composition profile is very similar for QDs capped by GaAs, with an In content comprised between 62% and 35%. The In core presents an inverted-triangle shape as it has been already reported elsewhere.[26,27] Figure 4 shows plan view at lower magnification and cross-sectional images of QDs capped by GaAs. The dot density of 17×10^8 dots/cm^2 is similar to the density measured by AFM on this sample. The QDs have a square base and a mean width of 37.5 nm (36 nm) with a standard deviation of 0.3 nm (1.4 nm) along the ⟨100⟩ (⟨010⟩) axis, respectively. This shows a very good size homogeneity. On the other hand we observe that about 30% of the QDs are dislocated and formed large clusters with nonuniform shape as we can see on Fig. 4(b). QD size appears to reach a critical value above

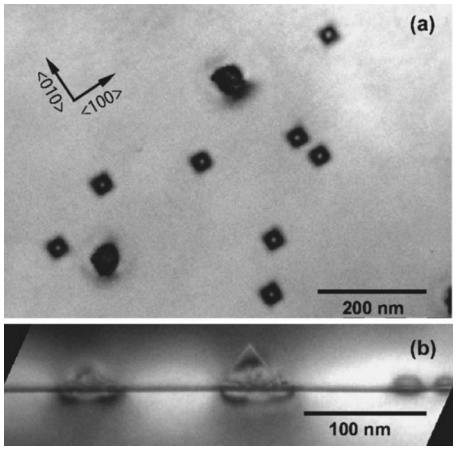

FIG. 4. (a) Plan view and (b) cross section images of QDs grown at low InAs growth rate (0.0015 ML/s) and capped by GaAs.

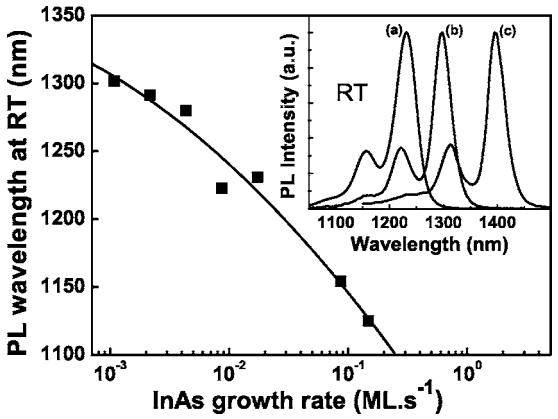

FIG. 5. RTPL emission wavelength as a function of InAs growth rate. The solid-thick line is a guide to the eye. Inset: normalized PL spectra at RT of 2.1-ML-thick, GaAs-capped InAs QDs grown at (a) 0.015 ML/s, (b) 0.0015 ML/s, (c) 2.1-ML-thick, InGaAs-capped InAs QDs grown at 0.0015 ML/s.

which plastic relaxation happens. Then, under these growth conditions, attachment of adatoms to existing islands is favored as opposed to nucleation of new islands, even if it leads to the formation of relaxed clusters. The self-size-limiting effect that has been observed in Refs. 28 and 29 here seems to be overcome by faster aggregation of adatoms.

Lastly, we note that the formation of these large clusters may also contribute to the abrupt decrease of the dot density observed in Fig. 1(b), by consuming In adatoms.

IV. PHOTOLUMINESCENCE SPECTROSCOPY OF QD ELECTRONIC STATES

In this section, we investigate the radiative properties of the QD electronic states, and particularly the role of the WL by optical spectroscopy. PL measurements have been performed at room temperature (RT) and low temperature (LT) on QDs grown at different InAs growth rates and capped by GaAs or InGaAs layer. Figure 5 presents the variation of the RTPL peak emission wavelength with InAs growth rate. The inset shows PL emission spectra of QDs capped by GaAs and InGaAs at RT. Ground state (GS) and first excited state (ES) signals are clearly distinguishable. We observe a strong redshift with decreasing growth rate. This can be related to a higher confinement energy due to a larger size and a higher In content of QDs grown at low growth rate.[30] Spectra (b) and (c) present a full width at half maximum (FWHM) value around 25 meV which confirms the remarkable size homogeneity observed on TEM images. The InGaAs-capped sample presents a PL peak centered at 1400 nm, redshifted by 100 nm as compared to the GaAs-capped sample, due to the increased QD height as observed by TEM. At LT, the PL peak shifts to ~1300 nm, which is a target wavelength for single-photon emission. Indeed, emission from single excitons and anticorrelation was measured from QDs grown in these conditions.[8,9]

In very low density QDs, the filling behavior of QD states for increasing pump power is presumably different due to the low density of states. Moreover, it may be argued that the large interdot distance increases the capture time from the WL to the QDs, creating a "capture bottleneck" and reducing the radiative efficiency. In the following we address these issues by continuous-wave and time-resolved PL experiments on different areal densities, as a function of excitation power. Figures 6(a)–6(c) report PL spectra measured at LT on GaAs-capped QDs grown at 0.015, 0.0015, and 0.0007 ML/s, respectively, at different excitation intensities. The GS and the two first ES signals are well separated. The QDs with lower areal density present a saturation of the GS intensity and an increase of the ES and WL intensities at lower pump powers than for the higher-density QDs due to the lower number of states. As expected, the saturated GS intensity also increases with the areal density.

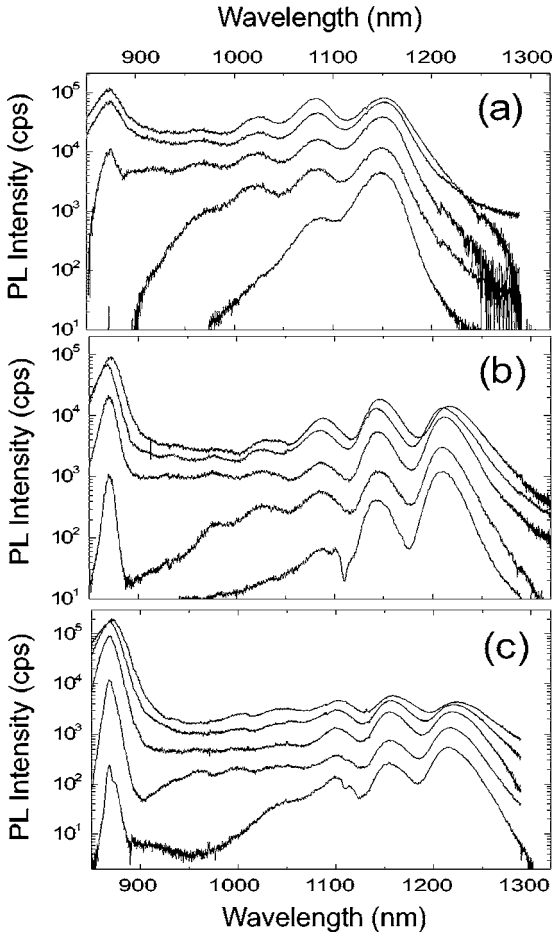

FIG. 6. PL emission at 12 K from GaAs-capped QDs grown with different InAs growth rates: (a) 0.015 ML/s, (b) 0.0015 ML/s, and (c) 0.0007 ML/s. Excitation intensity varies between 900 and 300 kW cm^{-2}.

From these spectra we extract the evolution of the WL emission wavelength for different InAs growth rates presented on Fig. 7(a). We observe a redshift of about 12 nm between low and high growth rates which could be due to a reduced WL thickness at low growth rate. This suggests that mass transport from WL to the QDs is more important at low growth rates. The emission wavelength of the 2D layer (WL+capping layer) of LDQDs covered by InGaAs layer, also shown (black rectangle) in Fig. 7(a), is strongly redshifted by about 65 nm, due to the increasing effective well thickness.

We now turn to the investigation of capture from WL to QDs for low areal densities. In Fig. 6, the WL emission is

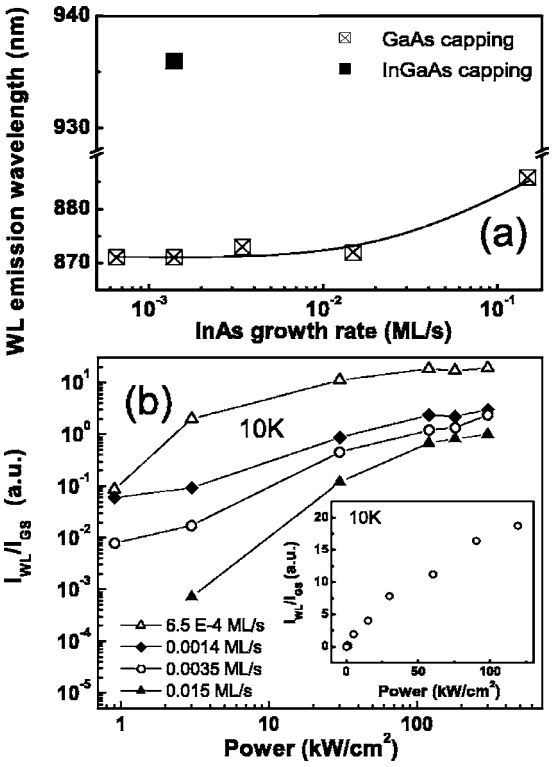

FIG. 7. Wetting layer emission wavelength as function of the InAs growth rate. The solid line is a guide to the eye. (b) Ratio between WL and GS PL integrated intensities at different InAs growth rate and as function of excitation power. Inset: Ratio between WL and GS PL integrated intensities as function of excitation power on the sample with InGaAs capping layer, on a linear scale.

clearly more intense for low-density samples. Figure 7(b) shows the ratio of WL to GS integrated intensities as a function of pump power density. The WL/ GS ratio increases with pump power for all samples, due to saturation of QD states, and is larger for low-density samples where saturation occurs at lower powers. However, as shown in the inset of Fig. 7 for the low-density (17×10^8 dots/cm^2) InGaAs-capped sample, the WL/GS ratio tends to be zero as the pump intensity is reduced. This proves that the capture time from the WL to the QD is still much shorter than the interband recombination time even in the lowest QD densities explored here. This result is important in view of the realization of efficient single-photon emitters, since a capture bottleneck in the WL would reduce the QD PL efficiency and strongly affect the emission properties of single excitons. Nevertheless, we note that a relatively strong WL emission is observed for excitation levels well below those corresponding to the saturation of QD confined states. This suggests a mechanism for carrier reexcitation from the QD state to the WL which is a function of carrier density (e.g., Auger effect). More detailed experimental investigations and modeling will be needed to fully elucidate this behavior.

Finally, we investigated the carrier relaxation and recombination processes in the LDQDs through TRPL measurements. The pump power was chosen so that the GS peak was far from saturation and the detection wavelength was set to correspond to the GS PL maximum using different bandpass filters. The inset of Fig. 8 shows the measured PL transients

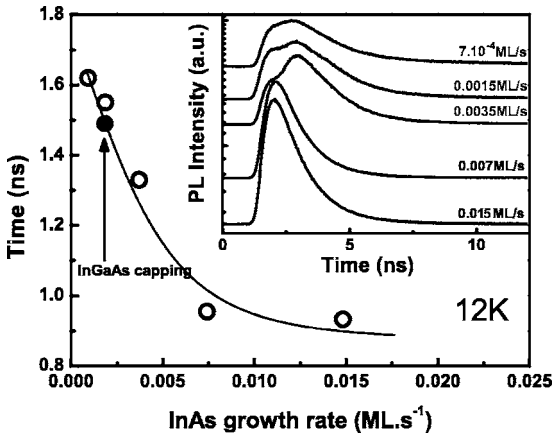

FIG. 8. Evolution of decay times as function of InAs growth rate. Inset: TRPL transients measured on QDs capped by GaAs. Excitation energy density: 1.7 μJ cm^{-2}.

for different growth rates at low temperature (12 K). The rise dynamics for the high growth rate sample is limited by the temporal resolution of our setup (600 ps); however, we observe an interesting delay of the GS luminescence for the low-density samples. As the GS is well below saturation at this excitation density, the delay cannot be related to carrier refilling from ES, as commonly observed in QD ensembles.[31] Furthermore, we observe that this delay disappears at low excitation density or when the sample temperature exceeds 150 K. We tentatively associate this complex GS rise dynamics to the presence of carriers in the WL which becomes more significant in low-density QDs. The initial part of the dynamic may be related to the emission of GS excitons in the presence of WL spectator carriers, which disappear at longer times, leaving the usual exciton decay. This hypothesis is supported by the observation (not shown) of WL emission (with ~400 ns decay time), under these experimental conditions.

The decay times were extracted by fitting the decay part of the TRPL with the convolution between a single-time constant exponential for the signal and the measured setup response function. They are presented on Fig. 8 as function of growth rate. The decay time is observed to increase with increasing QD size. The increase of PL decay time indicates a reduction of the oscillator strength, which is likely related to a reduced electron-hole wave function overlap for large QD diameter.[32]

V. TEMPERATURE DEPENDENCE

Finally, we investigated the temperature stability of LDQD PL emission. PL measurements at different temperatures have been performed on two samples with QDs grown at the same growth rate (0.0015 ML/s) capped by InGaAs or GaAs. The pump wavelength and the power density were fixed at 780 nm and 6 kW cm^{-2}, respectively. Figures 9 and 10 show the evolution of the GS peak energy, the FWHM, and the PL integrated intensity as a function of temperature. The peak shift is similar for both samples with a redshift of 64 meV between 10 and 300 K, as shown on Fig. 9(a). We fit this redshift with the empirical relation[33] for the temperature

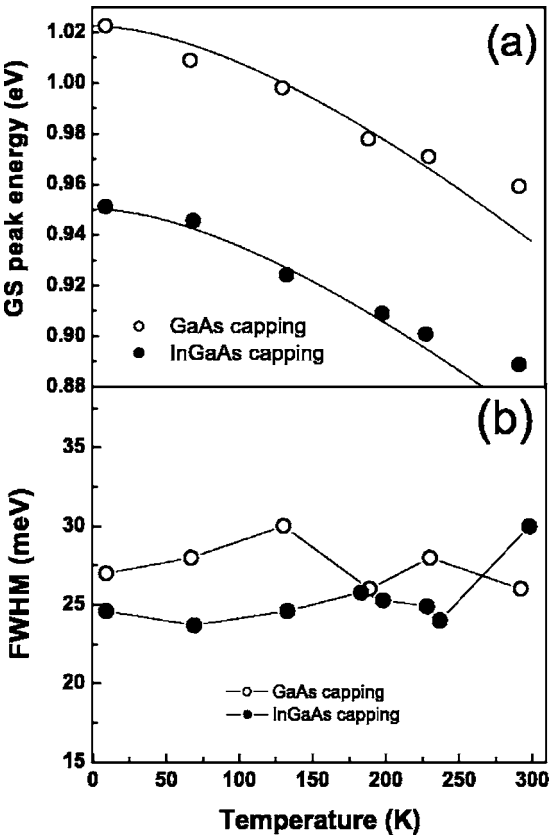

FIG. 9. (a) Evolution for different temperatures of the GS energy peak. The solid lines show the temperature dependence of the bulk $In_xGa_{(1-x)}As$ band gap with $x=0.35$ and 0.41, following Ref. 33. (b) Evolution of the FWHM of the GS peak.

dependence of $In_xGa_{(1-x)}As$ band gap, with $x=0.35$ and 0.41 for the GaAs-capped and InGaAs-capped QDs, respectively. For comparison, TEM measurements indicate a mean In composition of 50.4% and 50.6% for GaAs-capped and InGaAs-capped sample, respectively. In-content inhomogeneity in the QDs, which is not taken into account in Ref. 33, can explain this composition difference. Capping layer composition thus influences QD dimension rather than QD composition.

FWHM evolution with temperature is similar for the two

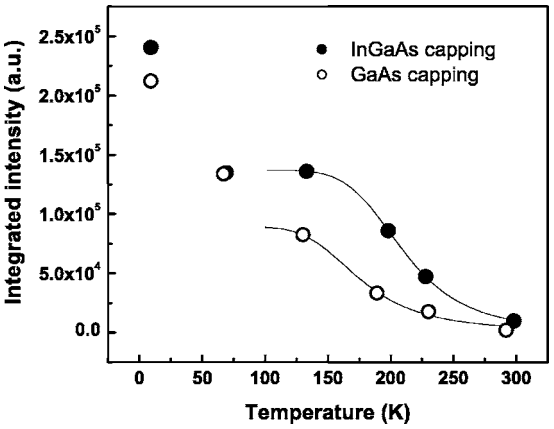

FIG. 10. Integrated intensity as a function of temperature for InGaAs- and GaAs-capped QDs grown at 0.0015 ML/s, under an excitation density of 6 kW cm^{-2}. Fitting curves are represented by the solid lines.

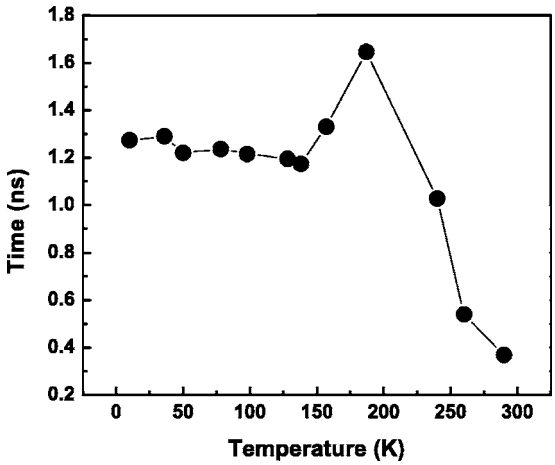

FIG. 11. Evolution of decay time for QDs capped by InGaAs as function of temperature. Excitation energy density: 6 $\mu J/cm^{-2}$.

different capping layers. Its overall variation is smaller than 5 meV (~20%) which highlights the high size homogeneity of the LDQDs.[34]

We observe on Fig. 10 that PL intensity quenches by a factor of 100 (25) for QDs capped by GaAs (InGaAs) between low and room temperatures. We note that the quenching is lower by using an InGaAs capping layer, although the carrier confinement is higher for QDs capped by GaAs. For $T>100$ K, the temperature dependence of the luminescence intensity can be expressed with a single activation energy E_a as

$$I \propto \frac{1}{1+B\exp(-E_a/kT)}.$$

The fits provide E_a values of 130 and 156 meV for QDs capped by GaAs and InGaAs, respectively. This activation energy is much smaller than the energy difference between the QD GS and the WL, so that the PL quenching cannot be attributed to the thermal escape of excitons to the WL, contrary to what is observed in smaller QDs.[35] Due to the absence of a confining heterostructure around the photoexcited GaAs region, the PL temperature dependence may also reflect the carrier diffusion to nonradiative states on the surface and in the substrate. In order to isolate the intrinsic nonradiative characteristics of QDs, we measured the QD carrier lifetime as a function of temperature. Figure 11 shows the measured lifetime at the GS energy of a sample containing LDQDs with InGaAs capping as a function of temperature. By comparison with Fig. 8, we used a higher excitation power in this experiment and we observe a shorter lifetime. This can be attributed to an enhancement of Auger recombination process with excitation density.[36] We observe that the lifetime is independent of temperature for $T<150$ K, increases up to 1.7 ns at 180 K, then decreases to 0.4 ns at RT. This type of behavior has already been reported and interpreted.[37–39] The temperature independence of the lifetime between 10 and 150 K (Ref. 40) is a consequence of the quantized energy structure. From this, we can deduce that the reduction of the luminescence intensity observed for temperatures below 100 K is due rather to carrier capture by defects before recombination in the QDs than to nonradiative

recombination in the QDs. The subsequent increase of the lifetime with temperature can be attributed to thermal population of a dark exciton state[41,42] consisting of an electron in the GS and a hole in the ES. At temperature above 200 K, the PL decay time drops due to the enhanced influence of nonradiative recombination channels, which confirms the existence of nonradiative recombination channels thermally activated for $T > 150$ K, as also observed in continuous-wave PL.

VI. CONCLUSION

Under extreme growth conditions, where In desorption rate is in competition with deposition rate, InAs/GaAs QDs with a very low density have been formed. They present the usual lens shape with a much larger size and higher In content than QDs grown at higher In deposition rate. TEM characterizations reveal a very good size homogeneity which results in a small and weakly temperature-dependent FWHM of the GS PL peak. PL investigations of QDs grown at different InAs growth rates and a study of the relative intensity of GS and WL signals show an efficient carrier capture mechanism into the QDs even for densities as low as few QDs/μm^2. Nevertheless, the effect of WL carriers in LDQDs at moderate excitation densities is evidenced in a complex PL rise dynamics which is for the moment not fully understood and should be completed by further investigations and modeling. Temperature dependence measurements performed on LDQDs capped by InGaAs show a good stability of their luminescence intensity and a lifetime evolution, at the GS energy, which is similar to those reported for higher-density QD samples.

These LDQDs thus present attractive characteristics for the realization of efficient single-photon emitters at telecommunications wavelength under both optical and electrical excitations. Additional investigations on the role of WL carriers in the recombinations of QD excitons will be needed to further validate this active material.

ACKNOWLEDGMENTS

We wish to acknowledge fruitful discussions with Professor Nicolas Grandjean. This work was supported by the Swiss National Science Foundation (NCCR Quantum photonics and "Professeur boursier" program) and the EU project "QAP."

[1]P. Michler, A. Kiraz, C. Becher, W. V. Schoenfeld, P. M. Petroff, L. Zhang, E. Hu, and A. Imamoglu, Science **290**, 2282 (2000).
[2]C. Santori, M. Pelton, G. Salomon, Y. Dale, and Y. Yamamoto, Phys. Rev. Lett. **86**, 1502 (2001).
[3]V. Zwiller, H. Blom, P. Jonsson, N. Panev, S. Jeppesen, T. Tsegaye, E. Goobar, M. Pistol, L. Samuelson, and G. Björk, Appl. Phys. Lett. **78**, 2476 (2001).
[4]K. Takemoto, Y. Sakuma, S. Hirose, T. Usuki, and N. Yokoyama, Jpn. J. Appl. Phys., Part 2 **43**, L349 (2004).
[5]T. Miyazawa, K. Takemoto, Y. Sakuma, S. Hirose, T. Usuki, N. Yokoyama, M. Takatsu, and Y. Arakawa, Jpn. J. Appl. Phys., Part 2 **44**, L620 (2005).
[6]G. Saint-Girons, N. Chauvin, A. Michon, G. Patriarche, G. Beaudoin, G. Brémond, C. Bru-Chevallier, and I. Sagnes, Appl. Phys. Lett. **88**, 133101 (2006).
[7]M. B. Ward, O. Z. Karimov, D. Unitt, Z. L. Yuan, P. See, D. G. Gevaux, A. J. Shields, P. Atkinson, and D. Ritchie, Appl. Phys. Lett. **86**, 201111 (2005).
[8]C. Zinoni *et al.*, Appl. Phys. Lett. **88**, 131102 (2006).
[9]B. Alloing *et al.*, Appl. Phys. Lett. **86**, 101908 (2005).
[10]P. B. Joyce, T. J. Krzyzewski, G. R. Bell, T. S. Jones, S. Malik, D. Childs, and R. Murray, Phys. Rev. B **62**, 10891 (2000).
[11]C. Monat, B. Alloing, C. Zinoni, L. Li, and A. Fiore, Nano Lett. **6**, 1464 (2006).
[12]F. Patella, F. Arciprete, M. Fanfoni, A. Balzarotti, and E. Placidi, Appl. Phys. Lett. **88**, 161903 (2006).
[13]D. Leonard, K. Pond, and P. M. Petroff, Phys. Rev. B **50**, 11687 (1994).
[14]Y. Tu and J. Tersoff, Phys. Rev. Lett. **93**, 216101 (2004).
[15]V. G. Dubrovskii, G. E. Cirlin, and V. M. Ustinov, Phys. Status Solidi B **241**, R42 (2004).
[16]C. A. Jeffrey, E. H. Conrad, R. Feng, M. Hupalo, C. Kim, P. J. Ryan, P. F. Miceli, and M. C. Tringides, Phys. Rev. Lett. **96**, 106105 (2006).
[17]M. C. Bartelt and J. W. Evans, Phys. Rev. B **46**, 12675 (1992).
[18]J. A. Venables, G. D. T. Spiller, and M. Hanbucken, Rep. Prog. Phys. **47**, 399 (1984).
[19]T. J. Krzyzewski and T. S. Jones, J. Appl. Phys. **96**, 668 (2004).
[20]C. Heyn, A. Boltz, T. Matlezopoulos, R. L. Johnson, and W. Hansen, J. Cryst. Growth **278**, 46 (2005).
[21]P. B. Joyce, T. J. Krzyzewski, G. R. Bell, and T. S. Jones, Appl. Phys. Lett. **79**, 3615 (2001).
[22]P. Offermans, P. M. Koenraad, R. Nötzel, J. H. Wolter, and K. Pierz, Appl. Phys. Lett. **87**, 111903 (2005).
[23]D. M. Bruls *et al.*, Appl. Phys. Lett. **81**, 1708 (2002).
[24]G. Patriarche, L. Largeau, and J.-C. Harmand, Appl. Phys. Lett. **84**, 203 (2004).
[25]A. Lemaitre, G. Patriarche, and F. Glas, Appl. Phys. Lett. **85**, 3717 (2004).
[26]N. Liu, J. Tersoff, O. Baklenov, A. L. Holmes, Jr., and C. K. Shih, Phys. Rev. Lett. **84**, 334 (2000).
[27]A. Lenz *et al.*, Appl. Phys. Lett. **81**, 5150 (2002).
[28]I. Mukhametzhanov, Z. Wei, R. Heitz, and A. Madhukar, Appl. Phys. Lett. **75**, 85 (1999).
[29]T. Kaizu and K. Yamaguchi, Jpn. J. Appl. Phys., Part 1 **40**, 1885 (2001).
[30]P. B. Joyce, T. J. Krzyzewski, G. R. Bell, T. S. Jones, S. Malik, D. Childs, and R. Murray, J. Cryst. Growth **227**, 1000 (2001).
[31]S. Raymond *et al.*, Phys. Rev. B **54**, 11548 (1996).
[32]L. Y. Karachinsky, S. Pellegrini, G. Buller, A. Shkolnik, N. Y. Gordeev, V. P. Evtikhiev, and V. B. Novikov, Appl. Phys. Lett. **84**, 7 (2004).
[33]S. Paul, J. B. Roy, and P. K. Basu, J. Appl. Phys. **69**, 827 (1991).
[34]K. Yamaguchi, T. Kaizu, K. Yujobo, and Y. Saito, J. Cryst. Growth **237**, 1301 (2002).
[35]S. Sanguinetti, M. Henini, M. Grassi Alessi, M. Capizzi, P. Frigeri, and S. Franchi, Phys. Rev. B **60**, 8276 (1999).
[36]D. Morris, N. Perret, and S. Fafard, Appl. Phys. Lett. **75**, 3593 (1999).
[37]A. Fiore, P. Borri, W. Langbein, J. M. Hvam, U. Oesterle, R. Houdré, R. P. Stanley, and M. Ilegems, Appl. Phys. Lett. **76**, 3430 (2000).
[38]F. Pulizzi, A. J. Kent, A. Patanè, L. Eaves, and M. Henini, Appl. Phys. Lett. **84**, 3046 (2004).
[39]F. Adler, M. Geiger, A. Bauknecht, D. Haase, P. Ernst, A. Dörnen, F. Scholz, and H. Schweizer, J. Appl. Phys. **83**, 1631 (1998).
[40]G. Wang, S. Fafard, D. Leonard, J. E. Bowers, J. L. Merz, and P. M. Petroff, Appl. Phys. Lett. **64**, 2815 (1994).
[41]W. Yang, R. R. Lowe-Webb, H. Lee, and P. C. Sercel, Phys. Rev. B **56**, 13314 (1997).
[42]M. Gurioli, A. Vinattieri, M. Zamfirescu, M. Colocci, S. Sanguinetti, and R. Notzel, Phys. Rev. B **73**, 085302 (2006).